

# Variational Methods for Discrete Surface Parameterization. Applications and Implementation.

vorgelegt von  
Dipl.-Math. techn. Stefan Sechelmann

von der Fakultät II - Mathematik und Naturwissenschaften  
der Technischen Universität Berlin  
zur Erlangung des akademischen Grades

Doktor der Naturwissenschaften  
– Dr. rer. nat. –

Promotionsausschuss

Vorsitzender: NN  
Gutachter/Berichter: Prof. Dr. Alexander I. Bobenko  
NN

Tag der wissenschaftlichen Aussprache: NN

Berlin, den 07. Januar 2013



# Contents

<b>Introduction</b>	<b>1</b>
<b>1 Uniformization of discrete Riemann surfaces</b>	<b>3</b>
1.1 Discrete Riemann surfaces . . . . .	3
1.2 Uniformization . . . . .	5
1.3 Variational principles for discrete metrics in $\mathbb{E}^2$ , $\mathbb{H}^2$ , and $\mathbb{S}^2$ . . . . .	6
1.4 Quotient spaces and fundamental domains . . . . .	6
1.4.1 The cut-graph and fuchsian groups . . . . .	7
1.4.2 Minimal presentation . . . . .	8
1.4.3 Separated handles . . . . .	8
1.4.4 Opposite sides identified . . . . .	8
1.4.5 Canonical Keen Polygons . . . . .	8
1.5 Uniformization of embedded genus $g = 0$ , $g = 1$ , and $g > 1$ surfaces . . . . .	8
1.6 Branched coverings of $\hat{\mathbb{C}}$ . . . . .	8
1.6.1 Elliptic curves . . . . .	8
1.6.2 The moduli space . . . . .	8
1.6.3 Numerical convergence analysis . . . . .	8
1.6.4 The modulus of the Wente torus . . . . .	8
1.6.5 Construction of hyperelliptic surfaces . . . . .	8
1.6.6 Weierstrass points on hyperelliptic surfaces . . . . .	8
1.6.7 Canonical domains . . . . .	10
1.6.8 Lawsons surface . . . . .	10
1.7 Uniformization of Schottky data . . . . .	10
1.7.1 Images of isometric circles . . . . .	10
1.7.2 Hyperelliptic data . . . . .	10
1.8 Conformal maps to $\hat{\mathbb{C}}$ . . . . .	10
1.8.1 Selection of Branch Data . . . . .	10

1.8.2	Examples . . . . .	10
1.9	Surfaces with boundary . . . . .	10
1.9.1	Variation of edge length . . . . .	10
1.9.2	Examples . . . . .	10
1.10	Conformal maps of planar domains . . . . .	10
1.10.1	Boundary conditions . . . . .	10
1.10.2	Comparison with examples of the Schwarz-Christoffel community . . . . .	10
<b>2</b>	<b>Variational Methods for Discrete Surface Parameterization</b>	<b>11</b>
2.1	Discrete quasiisothermic parametrizations . . . . .	11
2.1.1	Introduction . . . . .	11
2.1.2	Related Work . . . . .	14
2.1.3	Discrete quasiisothermic parameterization . . . . .	14
2.1.4	Minimization of the Functional . . . . .	16
2.1.5	Discrete S-isothermic surfaces . . . . .	21
2.1.6	Conclusions and Future Research . . . . .	25
2.1.7	A discrete S-isothermic ellipsoid and its dual surface . . . . .	26
2.2	Projective interpolation for arbitrary parameterizations . . . . .	26
2.3	A variational principle for discrete Tschebyshev nets . . . . .	28
2.3.1	Variational principle . . . . .	28
2.3.2	Energies . . . . .	28
2.3.3	Initialization and parameters . . . . .	29
2.3.4	Implementation . . . . .	29
<b>3</b>	<b>Discrete Differential Geometry - Software Packages</b>	<b>31</b>
3.1	JRWORKSPACE - A plug-in driven GUI library . . . . .	32
3.1.1	Plug-ins . . . . .	32
3.1.2	Gui elements . . . . .	32
3.1.3	JRWORKSPACE and JREALITY . . . . .	32
3.1.4	Building a <i>jrworkspace</i> application . . . . .	32
3.2	The JTEM libraries HALFEDGE and HALFEDGETOOLS . . . . .	32
3.2.1	The halfedge data structure and tools . . . . .	32
3.2.2	Data model and algorithms . . . . .	32
3.3	CONFORMALLAB - Conformal maps and uniformization . . . . .	32
3.3.1	Embedded surfaces . . . . .	32
3.3.2	Elliptic and hyperelliptic surfaces . . . . .	32
3.3.3	Schottky data . . . . .	32

3.3.4	Surfaces with boundary . . . . .	32
3.4	VARYLAB - Variational methods for discrete surfaces . . . . .	32
3.4.1	Functional plug-ins . . . . .	32
3.4.2	Implemented functionals and options . . . . .	32
3.4.3	Remeshing . . . . .	32
3.5	U3D - 3D content in presentations and online publications . . . . .	32
3.5.1	3D content in PDF documents . . . . .	32
3.6	Non-linear optimization with jPETSc/jTao . . . . .	32
3.6.1	A java wrapper for PETSc/Tao . . . . .	32
<b>Bibliography</b>		<b>33</b>
<b>Acknowledgements</b>		<b>37</b>



# List of Figures

1.1	Discrete surfaces from glued triangles . . . . .	3
1.2	Euclidean conformal equivalence . . . . .	4
1.3	Conformal equivalence of Euclidean and hyperbolic/spherical metrics . . . . .	5
1.4	Angles at a vertex . . . . .	6
1.5	Hyperbolic flat metric on a genus 2 surface and the axes of the associated hyperbolic motions. . . . .	7
1.6	Square with symmetric slit to the circle . . . . .	9
2.1	Quasiisothermic parameterization step-by-step . . . . .	12
2.2	Quasiisothermic parameterization: Examples . . . . .	13
2.3	A discrete isothermic parameterization. Angles between triangle edges and a curvature direction family are preserved by the map. . . . .	15
2.4	Curvature boundary conditions . . . . .	17
2.5	Parameterization of the ROOF model. The discrete curvature lines approximate curvature directions with high quality. See Section 2.1.4 for a discussion. . . . .	18
2.6	Parameterization quality plot . . . . .	20
2.7	S-isothermic meshes . . . . .	22
2.8	Labels for the touching-circles-functional at an edge. The circles touch if the ratio $\cot(\beta^i/2) / \cot(\beta^j/2)$ is equal on both sides of the edge. . . . .	22
2.9	The S-isothermic circle packing on the ROOF model in detail. . . . .	23
2.10	Convergence behavior of $E_S$ . . . . .	24
2.11	Non-trivial isometric deformations of a minimal surface. The edges of the dual surface are rotated to create a 1-parameter family of isometrically deformed surfaces with period $2\pi$ . The histogram shows the edge length error of the $90^\circ$ model when compared with the initial surface. The mean edge length deviation of this model is 1.28%. . . . .	25
2.12	Discrete S-isothermic ellipsoid . . . . .	26
2.13	Dual surface of discrete S-isothermic ellipsoid of Figure 2.12. . . . .	27

2.14	Linear (left) and circum circle preserving piece-wise projective (middle) interpolation at a cone-singularity of a coarse mesh (right) with vertices on a sphere. The parameterization is discrete conformal. . . . .	27
2.15	Linear (left) and piece-wise projective (middle) interpolation at a cone-singularity of a coarse mesh (right). The parameterization is not discrete conformal. . . . .	28
2.16	Different initialization shear angles for a conformal remesh. $30^\circ$ left, $0^\circ$ middle, and $-30^\circ$ right. . . . .	29



# Introduction



# Chapter 1

## Uniformization of discrete Riemann surfaces

The discrete uniformization theory presented here is based on the notion of discrete conformal equivalence of triangle meshes. The Euclidean definition was first considered by [Luo04], the variational principle and applications in computer graphics is due to [SSP08, Spr09, BPS10]. The notion of conformal equivalence of non-Euclidean metrics and corresponding variational principles were first defined in [BPS10]. [Guo11] investigate the gradient flow of this principle. Most of the material presented here can be found in [BSS].

### 1.1 Discrete Riemann surfaces

**Definition 1.** A discrete surface is a collection of triangles equipped with a metric of constant Gaussian curvature and geodesic edges. Triangles are glued along edges to form a surface.

By glueing triangles equipped with a metric of constant Gaussian curvature we obtain a surface that has constant curvature everywhere except for points where the metric has cone-like singularities (Figure 1.1). A discrete surface is called Euclidean for  $K = 0$ , hyperbolic for  $K < 0$ , and spherical if  $K > 0$ . Remark: In the latter we will use Gaussian curvature and curvature synonymously. Generically a discrete surface can have boundary components where triangles have not been glued. We consider this case in Section 1.10.



Figure 1.1: Discrete surfaces constructed from glued triangles of constant curvature. Euclidean, hyperbolic, and spherical. Bold edges are identified to create a cone-like singularity at the vertex.

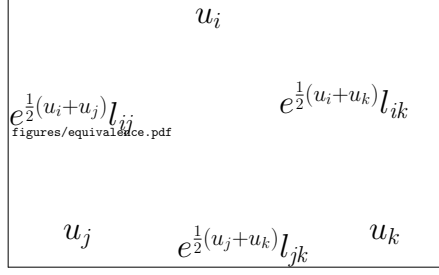


Figure 1.2: Two Euclidean triangles are discretely conformally equivalent if their edge lengths can be scaled by logarithmic factors  $u$  defined on vertices.

A discrete surface consists of vertices, edges, and faces  $S = (V, E, F)$ . We use single indices for denoting vertices, e.g.,  $i \in V$ , edges are denoted  $ij \in E$ , and faces  $ijk \in F$ .

**Definition 2.** *The map  $l : E \rightarrow \mathbb{R}$  of triangle edge lengths of a discrete surface is called a discrete Euclidean, hyperbolic, or spherical metric respectively.*

As in the smooth theory we define what it means for a metric to be conformally equivalent to another metric.

**Definition 3.** *A discrete Euclidean metric with edge lengths  $l$  is discretely conformally equivalent to the discrete Euclidean metric  $\tilde{l}$  if there is a function  $u : V \rightarrow \mathbb{R}$  such that for all edges  $ij \in E$  it is*

$$l_{ij} = e^{\frac{1}{2}(u_i + u_j)} \tilde{l}_{ij} \quad (1.1)$$

This definition is motivated by the smooth theory of Riemann surfaces where two metrics  $g$  and  $\tilde{g}$  on a 2-manifold  $M$  are conformally equivalent if there is a smooth function  $u : M \rightarrow \mathbb{R}$  with

$$g = e^{2u} \tilde{g}.$$

Every discrete Euclidean metric is discretely conformally equivalent to a corresponding discrete hyperbolic or discrete spherical metric by the following

**Definition 4.** *A discrete Euclidean metric  $l$  and a discrete hyperbolic or discrete spherical metric  $\tilde{l}$  are discretely conformally equivalent if for all edges  $ij \in E$*

$$l_{ij} = 2 \sinh \frac{\tilde{l}_{ij}}{2} \quad (1.2)$$

$$l_{ij} = 2 \sin \frac{\tilde{l}_{ij}}{2} \quad (1.3)$$

for  $\tilde{l}$  hyperbolic or spherical respectively (see Figure 1.3).

Literally this means that in the spherical case if a triangle is fit onto the sphere the conformally equivalent spherical lengths are the lengths of spherical geodesics connecting the triangle vertices. The same intuition holds on the upper sheet of the two-sheeted unit hyperboloid for hyperbolic triangles.

Combining Equations 1.1 and 1.2/1.3 we can define conformal equivalence of Euclidean and hyperbolic/spherical triangulations via transitivity of equivalence.

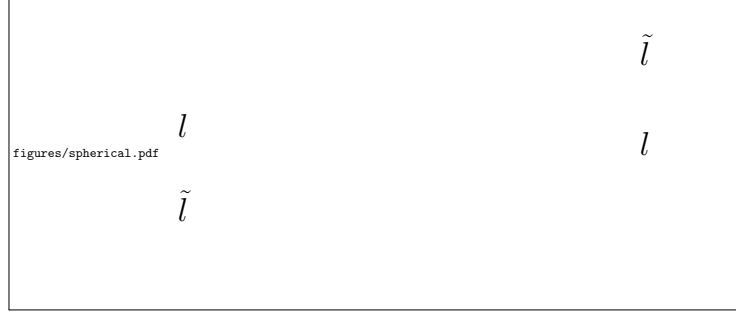


Figure 1.3: Relations between hyperbolic/spherical lengths  $\tilde{l}$  and corresponding Euclidean edge lengths  $l$ . See Definition 4.

With this general notion of conformal equivalence of Euclidean, hyperbolic, and spherical metrics we can now define discrete Riemann surfaces.

**Definition 5.** *A discrete Riemann surface is an equivalence class of discretely conformally equivalent metrics.*

If one restricts the equivalence class to either Euclidean, hyperbolic, or spherical metrics the length cross-ratio  $\text{lcr}_{ij}$  at edge  $ij$  with opposite vertices  $k$  and  $m$  is a conformal invariant. Note that this definition depends on the orientation of the surface.

$$\text{lcr}_{ij} = \frac{l_{ik}l_{jm}}{l_{mi}l_{kj}} \quad (1.4)$$

## 1.2 Uniformization

We can now state the uniformization problem: *Given a discrete Riemann surface, find a metric of constant curvature without cone singularities.*

This means that the angles  $\alpha_{jk}^i$  of Euclidean, hyperbolic, or spherical triangles around each vertex  $i \in V$  sum up to  $2\pi$  (Figure 1.4). A discrete surface with a cone-like singularity free metric has constant curvature everywhere.

As in the smooth case we expect to find a discrete metric with zero Gaussian curvature for tori, a constant negative curvature metric for surfaces with genus  $g > 1$ , and a metric with positive constant curvature for spheres. In the latter we will normalize the curvature of the target spaces to have constant Gaussian curvature 0,  $-1$ , or 1.

In this work we calculate discrete uniformizations as minimizers of functionals that fit the target geometry. The variational description of the uniformization problem then amounts to finding a critical point of the functional  $E(u)$  where

$$\frac{\partial E}{\partial u_i} = 2\pi - \sum_{ijk \ni i} \alpha_{jk}^i. \quad (1.5)$$

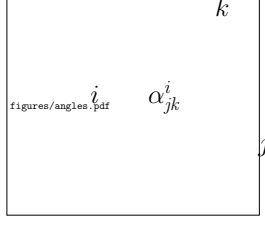


Figure 1.4: Angles at a vertex

### 1.3 Variational principles for discrete metrics in $\mathbb{E}^2$ , $\mathbb{H}^2$ , and $\mathbb{S}^2$

Construction of discrete flat metrics. A discrete Euclidean flat metric is the minimizer of a convex functional.

$$\lambda_{ij} := 2 \log l_{ij} \quad (1.6)$$

$$\tilde{\lambda}_{ij} := \lambda_{ij} + u_i + u_j \quad (1.7)$$

$$f_{Euc}(u_i, u_j, u_k) := \alpha_i \tilde{\lambda}_{jk} + \alpha_j \tilde{\lambda}_{ki} + \alpha_k \tilde{\lambda}_{ij} + 2(\mathcal{I}(\alpha_i) + \mathcal{I}(\alpha_j) + \mathcal{I}(\alpha_k)) \quad (1.8)$$

**Definition 6.**

$$E_{Euc}(u) := \sum_{ijk \in F} \left( f_{Euc}(u_i, u_j, u_k) - \frac{\pi}{2} (\tilde{\lambda}_{jk} + \tilde{\lambda}_{ki} + \tilde{\lambda}_{ij}) \right) + \sum_{i \in V} \Theta_i u_i \quad (1.9)$$

This definition and the derivatives can be found in [BPS10]

For the hyperbolic case  $\lambda$  and  $\tilde{\lambda}$  are defined as before. Further define

$$\beta_i := \frac{1}{2} (\pi + \alpha_i - \alpha_j - \alpha_k) \quad (1.10)$$

$$\beta_j := \frac{1}{2} (\pi - \alpha_i + \alpha_j - \alpha_k) \quad (1.11)$$

$$\beta_k := \frac{1}{2} (\pi - \alpha_i - \alpha_j + \alpha_k) \quad (1.12)$$

$$f_{Hyp}(u_i, u_j, u_k) := \beta_i \tilde{\lambda}_{jk} + \beta_j \tilde{\lambda}_{ki} + \beta_k \tilde{\lambda}_{ij} \quad (1.13)$$

$$+ \mathcal{I}(\alpha_i) + \mathcal{I}(\alpha_j) + \mathcal{I}(\alpha_k) + \mathcal{I}(\beta_i) + \mathcal{I}(\beta_j) + \mathcal{I}(\beta_k) \quad (1.14)$$

$$+ \mathcal{I} \left( \frac{1}{2} (\pi - \alpha_i - \alpha_j - \alpha_k) \right) \quad (1.15)$$

**Definition 7.**

$$E_{Hyp}(u) := \sum_{ijk \in F} \left( f_{Hyp}(u_i, u_j, u_k) - \frac{\pi}{2} (\tilde{\lambda}_{jk} + \tilde{\lambda}_{ki} + \tilde{\lambda}_{ij}) \right) + \sum_{i \in V} \Theta_i u_i \quad (1.16)$$

### 1.4 Quotient spaces and fundamental domains

Every Riemann surface  $R$  has a universal cover  $X$ , i.e., a simply connected covering space and a corresponding covering map. A metric of constant curvature on a compact 2-manifold can be realized as the quotient of the universal cover over a uniformizing group.



Figure 1.5: Hyperbolic flat metric on a genus 2 surface and the axes of the associated hyperbolic motions.

Triangulated surfaces of genus  $g \geq 2$  without boundary can be equipped with a discretely conformally equivalent flat hyperbolic metric [BPS10]. By flat hyperbolic metric we mean that the edge length are hyperbolic and for any vertex the angle sum is  $2\pi$ . To realize this metric in the hyperbolic plane e.g. in the Poincaré disk model one has to introduce cuts along a basis of the homotopy. This creates a simply connected domain in  $\mathbb{H}^2$ . Matching cut paths are related by a hyperbolic motion i.e. the Möbius transformations that leave the unit disk invariant (Figure 1.5).

#### 1.4.1 The cut-graph and fuchsian groups

*Want so say here: the number of transformations generated by the mapping of corresponding edges equals the number of path segments in the homotopy-cut-graph. They generate a fuchsian group with #vertices relations*

**1.4.2 Minimal presentation****1.4.3 Separated handles****1.4.4 Opposite sides identified****1.4.5 Canonical Keen Polygons****1.5 Uniformization of embedded genus  $g = 0$ ,  $g = 1$ , and  $g > 1$  surfaces****1.6 Branched coverings of  $\hat{\mathbb{C}}$** 

In this section we discuss surfaces that arise as branched coverings of  $\hat{\mathbb{C}}$ . A Riemann surface that can be represented as a double cover of  $\hat{\mathbb{C}}$  is called elliptic for  $g = 1$  and hyperelliptic for  $g > 1$  [Jos07, p. 235].

Let  $\lambda_1, \dots, \lambda_{2g+2} \in \hat{\mathbb{C}}$ ,  $\lambda_i \neq \lambda_j \forall i \neq j$ . The algebraic curve

$$C = \{(z, w) \in \mathbb{C}^2 \mid w^2 = \prod_{i=1}^{2g+2} (z - \lambda_i)\} \quad (1.17)$$

is a one dimensional complex manifold. A branched double cover of  $\hat{\mathbb{C}}$  is the projection  $\pi : C \rightarrow \mathbb{C}$ ,  $C \ni (z, w) \mapsto z$ . A discrete branched cover of  $\hat{\mathbb{C}}$  is a triangulation of  $\pi(C)$  with vertices at  $\lambda_i$ .

**1.6.1 Elliptic curves****1.6.2 The moduli space****1.6.3 Numerical convergence analysis****1.6.4 The modulus of the Wente torus****1.6.5 Construction of hyperelliptic surfaces**

Any hyperelliptic Riemann surface can be expressed as an algebraic curve of the form

$$w^2 = \prod_{i=1}^{2g+2} (z - \lambda_i) \quad g \geq 1, \quad \lambda_i \neq \lambda_j \forall i \neq j.$$

Here  $\lambda_i$  are the branch points of the doubly covered Riemann sphere.

**1.6.6 Weierstrass points on hyperelliptic surfaces**

A hyperelliptic surface comes together with a holomorphic involution  $h$  called the hyperelliptic involution. The branch points are fixed points under this transformation. For a hyperelliptic





Figure 1.6: Square with symmetric slit to the circle

algebraic curve it is  $h(\mu, \lambda) = (-\mu, \lambda)$

### 1.6.7 Canonical domains

### 1.6.8 Lawsons surface

## 1.7 Uniformization of Schottky data

### 1.7.1 Images of isometric circles

### 1.7.2 Hyperelliptic data

## 1.8 Conformal maps to $\hat{\mathbb{C}}$

### 1.8.1 Selection of Branch Data

### 1.8.2 Examples

## 1.9 Surfaces with boundary

### 1.9.1 Variation of edge length

### 1.9.2 Examples

## 1.10 Conformal maps of planar domains

### 1.10.1 Boundary conditions

### 1.10.2 Comparison with examples of the Schwarz-Christoffel community

## Chapter 2

# Variational Methods for Discrete Surface Parameterization

### 2.1 Discrete quasiisothermic parametrizations

This work is joint with Thilo Rörig and Alexander Bobenko and was published in [SRB12]

*Abstract:* In architecture the quality of a quad-mesh depends on the shape of the individual quadrilaterals. The ideal shape from an architectural point of view is the planar square or rectangles with fixed aspect ratio. A parameterization that divides a surface into such shapes is called isothermic, i.e., angle-preserving and curvature-aligned. Such a parameterization exists only for the special class of isothermic surfaces. We extend this notion and introduce quasiisothermic parameterizations for arbitrary triangulated surfaces.

We describe an algorithm that creates quasiisothermic meshes. Interestingly many surfaces appearing in architecture are close to isothermic surfaces, namely those coming from form finding methods and physical simulation. For those surfaces our method works particularly well and gives a high quality and robust mesh layout. We show how to optimize such meshes further to obtain disk packing representations. The quadrilaterals of these meshes are planar and possess touching incircles.

#### 2.1.1 Introduction

A key problem in architectural geometry is to convert surfaces created by form finding methods, physical simulation, or manual modeling to quadrilateral meshes, which are preferred for glass-steel structures. There are many possible quad-meshes that approximate a given shape and we study those that consist of principle-curvature-aligned conformal squares (see Fig. 2.2). Not all surface shapes can be approximated by such meshes. A smooth analog of a surface with this property is called an isothermic surface. These surfaces admit conformal curvature line parameterizations, i.e., angle-preserving parameterizations aligned with the principle curvature directions. Their discrete counterpart are so-called S-isothermic meshes. These meshes have the additional property that neighboring quadrilaterals possess touching incircles (see Fig. 2.7).

The class of isothermic surfaces comprises, for example, constant mean curvature surfaces. Roofs



Figure 2.1: The algorithmic steps of this paper: For a triangulated surface we calculate texture coordinates by solving a boundary value problem for principle curvature directions on boundary edges (checker board texture and red directions). The edges of the corresponding quad mesh align with the curvature directions (red crosses). The mesh is then optimized towards planar quads with touching incircles.

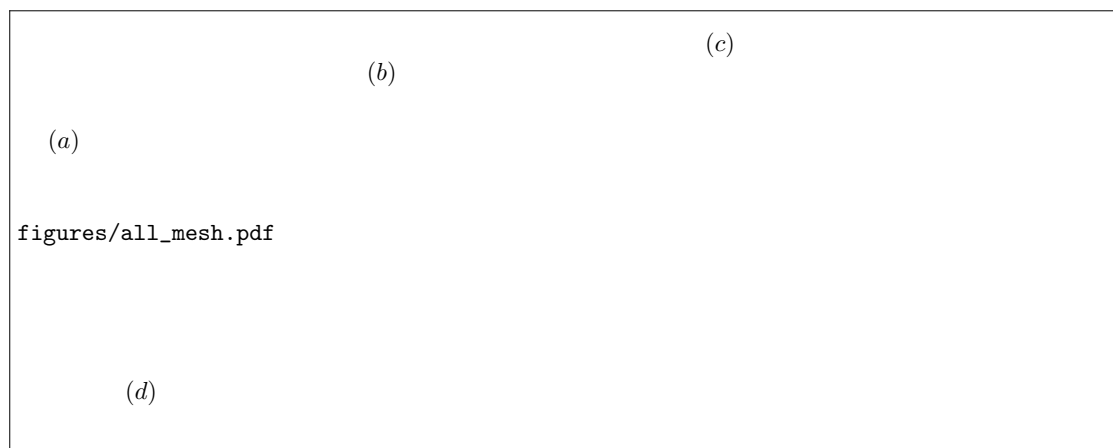


Figure 2.2: The surface examples of this paper. All have been parameterized and remeshed. (a) The TEASER surface is the minimizer of a spring energy with a smooth fixed boundary curve. (b) A MINIMAL surface with polygonal boundary curve. (c) DOME: Part of a NURBS surface exhibiting positive curvature and two curvature field singularities. (d) ROOF structure with planar boundary curve and regions of positive and negative curvature.

that act shell-like turn out to have almost constant mean curvature. These are the kinds of surfaces that initiated our study of conformal curvature line parameterizations in the architectural context. Both conformality and alignment with curvature lines are favorable properties for meshes.

The contributions of this paper are:

**Definition of quasiisothermic parameterizations:** We propose a definition of quasiisothermic parameterizations of triangle meshes. It is based on angles between curvature directions and edges of a triangle mesh. We define the quasiisothermic modulus that measures how isothermic a parameterization is. If this modulus is zero we obtain discrete isothermic parameterizations in the sense of our definition.

**Parameterization Algorithm:** We give an algorithm that creates quasiisothermic parameterizations based on discrete conformal maps of triangle meshes to the plane. This approach is build on top of the conformal mapping technique of [SSP08]. We inherit the speed and superior projective mapping properties of their parameterizations.

**Variational principle for circle packing quad-meshes:** The obtained parameterizations are used for remeshing and we optimize quadrilaterals to have touching incircles by minimizing a novel energy. These S-isothermic meshes have been studied in discrete differential geometry and possess some remarkable properties, e.g., minimal S-isothermic surfaces may be deformed isometrically retaining the same Gauß map.

The rest of the paper is organized as follows: Section 2.1.2 gives an overview of existing parameterization schemes and their relation to our approach. We also give reference to the related mathematical literature in discrete differential geometry. In Section 2.1.3 we define quasiisothermic parameterizations and a corresponding quality measure. In Section 2.1.4 we describe an algorithm to obtain quasiisothermic parameterizations with small modulus. We describe the connection to discrete conformal maps and discuss how we deal with singularities. A variational principle to generate S-isothermic meshes is presented in Section 2.1.5. At the end of the section

we show the effect of our optimization on several examples from different classes of surfaces. In the final Section 2.1.6 we sum up the results and propose extensions and enhancements subject to further research.

### 2.1.2 Related Work

There has been considerable work on conformal parameterizations as well as on curvature line parameterizations related to our quasiisothermic scheme. We can only give a selection of previous work here. For a general background on mesh parameterization we refer to the surveys by [FH05] and [SPR06].

Our algorithmic approach is based on the discrete conformal equivalence of triangle meshes introduced in [SSP08] (see [BPS10] for the mathematical background). The convex functional optimized in Springborn *et al.* constructs a conformally equivalent flat mesh for specified boundary conditions and singularities. Our work is related to [SdS01]. They aim for conformal parameterizations and express this by the additional constraint, that triangle angles have to be close to the original ones on the surface. For discrete isothermic parameterizations the definitions coincide.

Parameterizations aligning with lines of principle curvature were constructed by [ACSD<sup>+</sup>03]. Their method involves the integration of curvature vector fields and does not include an optimization towards conformality. Global parameterizations following arbitrary frame fields (including in particular principle curvature fields) are constructed in [KNP07]. They use discrete Hodge decomposition and harmonic vector fields to obtain a globally consistent parameterization. Their QuadCover algorithm can deal with surfaces of arbitrary genus and treats singularities using a suitable branched cover. Both algorithms cover arbitrary triangulated surfaces and implementations are highly complex.

The use of variational principles to enforce desired properties such as planarity of quadrilateral faces has been successfully used in architectural geometry. [LPW<sup>+</sup>06] propose an algorithm to optimize a quadrilateral mesh to become planar and even conical. [PSB<sup>+</sup>08] use functionals to approximate freeform surfaces with single curved panels. The energy minimized in Section 2.1.5 is a combination of a new functional with an energy recently described by [SHWP09]. They construct circle packing triangle meshes that approximate a given surface by minimizing a combination of energies. Discrete S-isothermic minimal surfaces are defined in terms of their Gauß map in [BHS06]. This Gauß map is a Koebe polyhedron with edges tangent to a sphere. These Koebe polyhedra also occur in the study of edge offset meshes by [PLW<sup>+</sup>07], which again use a variational approach to obtain support structures. Another parametrization technique creating quad-dominant meshes guided by conjugate parameter directions is given by [ZSW10]. Their algorithm includes a level set approach to circumvent the integration of a vector field.

The notion of discrete S-isothermic meshes was introduced in the mathematical context by [BP99] as a special class of quad meshes. The mathematical theory of these meshes has since then been an active field of research in discrete differential geometry. A good overview of the recent development and literature can be found in the book [BS08].

### 2.1.3 Discrete quasiisothermic parameterization

In this section we introduce the notion of quasiisothermic parameterizations and the corresponding quality measure.

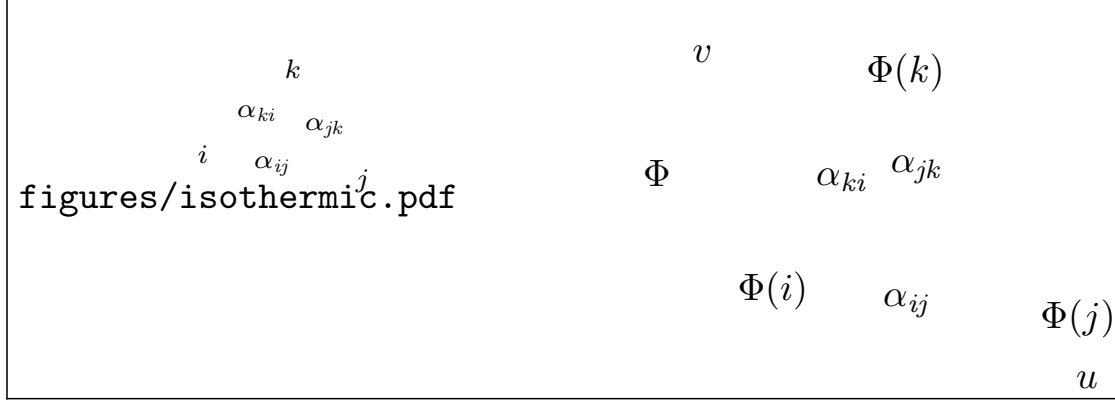


Figure 2.3: A discrete isothermic parameterization. Angles between triangle edges and a curvature direction family are preserved by the map.

### Discrete parameterizations

Let  $M = (V, E, F)$  be a triangle mesh. The elements of  $V$  are the vertices of the mesh denoted by simple indices  $i \in V$ . Edges are denoted by double indices  $ij \in E$ , and faces are denoted  $ijk \in F$ . A triangulated surface is a map  $S : V \rightarrow \mathbb{R}^3$ ,  $i \mapsto (x_i, y_i, z_i)$ . We call a map  $\Phi : V \rightarrow \mathbb{R}^2$ ,  $i \mapsto (u_i, v_i)$  a *discrete parameterization* of the surface  $S$ . We only consider orientable surfaces and parameterizations that preserve the orientation of the triangles with respect to the canonical orientation of  $\mathbb{R}^2$ .

The next definition connects arbitrary parameterizations with certain directions tangent to the surface  $S$ , e.g., curvature directions. Such a direction is encoded as an angle per edge.

**Definition 8.** Let  $\alpha : E \rightarrow ]-\frac{\pi}{2}, \frac{\pi}{2}]$ ,  $ij \mapsto \alpha_{ij}$  be a map that assigns an angle to each edge. A discrete parameterization  $\Phi : V \rightarrow \mathbb{R}^2$ ,  $i \mapsto (u_i, v_i)$  is called a discrete parameterization with  $\alpha$  if

$$\tan \alpha_{ij} = \frac{u_i - u_j}{v_i - v_j} \quad (2.1)$$

for all edges of the mesh.

In other words, in a parameterization with  $\alpha$  the image of an edge  $ij \in E$  under the map  $\Phi$  encloses the prescribed angle  $\alpha_{ij}$  with the  $v$ -axis of the parameter space. One could equally use the  $u$ -axis here.

### Quasiisothermic parameterizations

Our main example of a parameterization with an angle function  $\alpha$  comes from  $\alpha$  defined by the curvature directions of a surface  $S : V \rightarrow \mathbb{R}^3$  (see Fig. 2.3). For a triangulated surface curvature directions and magnitudes can be calculated and assigned to edges. This is usually done by averaging curvature information over neighborhoods of points on the surface [CSM03]. A discrete parameterization with angle function  $\alpha$  stemming from the curvature direction field is then called a *discrete isothermic parameterization*. Indeed, the latter is just a curvature line parameterization. In our case the curvature directions are mapped to the coordinate directions

in the  $(u, v)$ -plane. The map can be treated as conformal: Angles between edges and curvature directions are preserved.

Generic surfaces do not allow for isothermic parameters (those admitting isothermic parameterizations are called isothermic surfaces). Therefore we do not expect a parameterization with given  $\alpha$  to exist in general. To be able to deal with arbitrary surfaces we introduce the notion of discrete quasiisothermic parameterization. The idea is to obtain a parameterization with angles  $\tilde{\alpha}$  as close to the curvature directions  $\alpha$  as possible. Let

$$Q^\alpha(ij) = |\alpha(ij) - \tilde{\alpha}(ij)| \quad (2.2)$$

where  $\tilde{\alpha}(ij)$  is angle the between the  $v$ -axis and the edge  $ij$  in parameter space.

**Definition 9.** We call a discrete parameterization  $\Phi$  with angle function  $\alpha$  quasiisothermic with modulus  $Q \in \mathbb{R}_+$  if

$$Q^\alpha(ij) \leq Q \quad (2.3)$$

for all edges  $ij \in E$ .

The motivation for this measure of quasiisothermicity is the following: If  $Q$  is small the directions of principle curvature on the surface are almost tangent to the parameter lines of the parameterization. For a modulus of zero we have an in a sense angle preserving map where edges enclose the same angles with the coordinate axes in parameter space as with curvature directions on the surface. We will now create parameterizations that have small  $Q$ .

### 2.1.4 Minimization of the Functional

In this section the surface  $M$  is a triangulated surface with one boundary component. We will now construct a function  $\Phi$  that has zero approximation error  $Q^\alpha$  at boundary edges and is a discrete conformal map in the sense of [SSP08] in the interior of the surface. We argue under which circumstances this leads to nice behaviour in the interior. We start by briefly introducing discrete conformal maps and the boundary conditions we need for our purposes.

#### Discrete conformal maps

We recall the definition by Springborn *et al.* of discrete conformal maps via conformal equivalence of triangle meshes. It is stated in terms of lengths of the surface edges and corresponding parameter edges in the  $(u, v)$ -plane.

**Definition 10.** A discrete parameterization  $\Phi$  is conformal if there exists a function  $\mu : V \rightarrow \mathbb{R}$ ,  $i \mapsto \mu_i$  such that the following condition for the edge lengths  $l_{ij}$  on the surface and  $\tilde{l}_{ij} = \|\Phi(i) - \Phi(j)\|$  in parameter space holds

$$\tilde{l}_{ij} = \mu_i \mu_j l_{ij}. \quad (2.4)$$

For a given triangle mesh there is a unique solution  $\mu$  that retains the boundary edge lengths. Another unique solution can be obtained by fixing the angles between consecutive boundary edges. These angles have to be chosen consistently obeying the Gauß-Bonnet relation (see the section about singularities).

The function  $\mu$  for a given triangle mesh can be found as the minimizer of a convex functional. Thus its computation is efficient. The resulting parameterization is created by a breadth-first



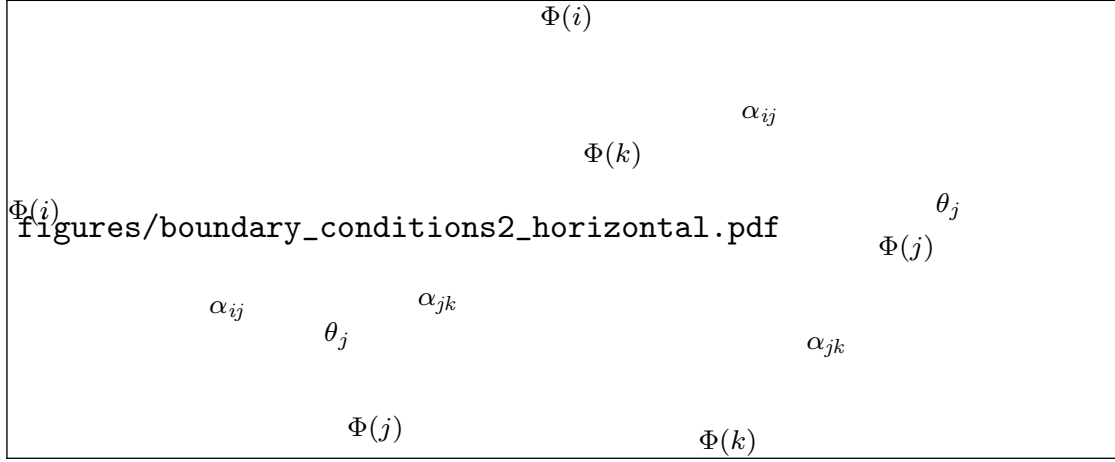


Figure 2.4: Curvature boundary conditions: In parameter space the interior angle  $\theta_j$  at the vertex  $\Phi(j)$  has to be chosen such that curvature directions given by angles  $\alpha_{ij}$  and  $\alpha_{jk}$  align with the  $v$ -axis. This choice is unique up to addition of  $k\pi$ . The above pictures show two possible layouts in the parameter plane depending on the interior angle sum on the surface.

layout that enumerates all triangles and assigns texture coordinates. In addition to boundary angles one can ask for solutions that contain special interior vertices where the sum of triangle angles is not equal to  $2\pi$  (see Fig. 2.1). These so-called cone points will be inserted at singularities of the parameterization.

### Curvature boundary conditions

Let  $\alpha : E \rightarrow ]-\frac{\pi}{2}, \frac{\pi}{2}]$  be an angle function derived from numerical curvature directions and the given surface orientation. Let  $ij \in E$  and  $jk \in E$  be two consecutive boundary edges with common vertex  $j$  and let  $\tilde{\theta}_j$  be the sum of interior triangle angles on the surface at this vertex. The direction of the edge  $\Phi(ij)$  (resp.  $\Phi(jk)$ ) is determined by the angle  $\alpha_{ij}$  (resp.  $\alpha_{jk}$ ), since the curvature directions encoded by the  $\alpha$ 's should align with the  $v$ -axis. The orientation of the surface (resp. the boundary edges) defines the angle  $\theta_j$  between the edges  $\Phi(ij)$  and  $\Phi(jk)$  up to addition of  $k\pi$  (see Fig. 2.4). To make the angle unique we require that the difference between the original surface angle  $\tilde{\theta}_j$  and the angle in the parameter plane  $\theta_j$  is as small as possible, i.e., choose  $k > 0$  as small as possible such that

$$|\underbrace{\angle(\Phi(ij), \Phi(jk))}_{\theta_j} + k\pi - \tilde{\theta}_j| \leq \pi/2.$$

See Figure 2.4 for an illustration of the alignment in the parameter plane. The angles  $\theta_j$  at boundary vertices serve as boundary conditions for the discrete conformal parameterization. A conformal parameterization with these boundary conditions will then have perfect alignment of curvature directions at the boundary.



Figure 2.5: Parameterization of the ROOF model. The discrete curvature lines approximate curvature directions with high quality. See Section 2.1.4 for a discussion.

### Singularities

There exists an analog of the smooth Gauß-Bonnet theorem for discrete surfaces that relates the Gaussian and the boundary curvature to the Euler characteristic. During parameterization we construct a metric that is flat everywhere except for cone singularities where positive or negative curvatures are introduced. For the purpose of curvature line parameterizations we can only have cone points with discrete curvatures of  $\pi$ ,  $0$ , or  $-k\pi$  at singularities of the curvature direction field. The Gaussian curvature  $\kappa_i$  at interior vertices  $i \in V_I$  is the angle defect, i.e.,  $\kappa_i = 2\pi - \theta_i$ , where  $\theta_i$  is the sum of the angles at the vertex  $i$ . For a boundary vertex  $j \in V_B$  the corresponding geodesic curvature is defined by  $\kappa_j^g = \pi - \theta_j$ . So if we split the vertex set  $V = V_B \cup V_I$  into boundary vertices  $V_B$  and interior vertices  $V_I$  the discrete Gauß-Bonnet theorem becomes:

$$\sum_{i \in V_I} \kappa_i + \sum_{j \in V_B} \kappa_j^g = 2\pi\chi, \quad (2.5)$$

where  $\chi$  is the Euler characteristic of the surface ( $\chi = 1$  for disks). Since all curvature directions at boundary edges in parameter space become parallel, the boundary curvature adds up to a multiple of  $\pi$ . If this sum happens to differ from  $2\pi$ , there must be singularities in the curvature field and we have to compensate the deficit at interior vertices to satisfy Equation (2.5). In Figure 2.5 the boundary curvature sum of the domain is  $4\pi$ . So by inspection of the curvature field in the interior of the surface we picked two singularities each of curvature  $-\pi$  to satisfy the Gauß-Bonnet equation. They correspond to cone points with angle  $3\pi$  in the parameterization.

### Implementation

The algorithm to compute a quasiisothermic parameterization with vanishing modulus at the boundary of the domain is the following:

1. Generate curvature directions and compute  $\alpha$  at the boundary
2. Calculate boundary angles  $\theta$  and pick singularities
3. Compute conformal parameterization with given  $\theta$ s
4. Perform remeshing
5. Remove cone point cuts

To estimate principle curvature fields we use the method of Cohen-Steiner and Morvan [CSM03], where the curvature tensor is averaged over a disk of a given radius centered at edge midpoints. Together with a fixed orientation of the surface this defines the angle function  $\alpha$ .

We deduce the angles  $\theta$  for the boundary vertices as described in Section 2.1.4. These angles are the boundary curvatures we plug into the algorithm of Springborn *et al.* to obtain a conformal parameterization. If necessary, we pick singularities for the curvature field at vertices and prescribe corresponding cone angles by inspection of the curvature direction field on the interior of the surface. A consistent singularity choice can easily be checked using Equation (2.5). By construction we can only process curvature fields with isolated singularities.

We layout the new edges in the parameter plane such that an arbitrary boundary edge  $\Phi(ij)$  intersects the  $v$ -axis in the desired angle  $\alpha_{ij}$ . By construction the intersection angles coincide with the prescribed  $\alpha$ 's for all boundary edges. The domain of parameterization can contain singularities, which are modeled as cone points with prescribed curvature. Therefore we have to cut along paths from the cone points to the boundary of the mesh. The layout overlaps if singularities with negative curvature are used. To create seamless parameter lines we use the rectification approach described in [SSP08].

Finally, we create a new mesh based on a regular  $(u, v)$ -grid in  $\mathbb{R}^2$ . The remeshing process is carried out as a subdivision step followed by some cleanup and regluing: We use the projective interpolation in the texture domain to increase the quality of the result. Previously cut paths from singularities to the boundary are sewed up to obtain the final remesh.

### Examples and quality

With the quasiisothermic modulus  $Q^\alpha$  on edges introduced in Equation (2.2) we are now able to measure the quality of our parameterizations.

There are two kinds of examples to consider: The first class of meshes stems from smooth surfaces that admit conformal curvature line parameterizations, i.e., triangulations approximating isothermic surfaces. The second class consists of arbitrary non-isothermic surfaces. For almost isothermic surfaces we expect our parameterization to reconstruct the isothermic coordinates up to numerical precision and hence  $Q^\alpha$  to be reasonably small. For non-isothermic surfaces we achieve the correct directions on the boundary but lack accuracy in the interior. In Table 2.1 we summarize the numerical results obtained from the surfaces of Figure 2.2.

**Isothermic surfaces.** The class of smooth isothermic surfaces contains surfaces of constant mean curvature, surfaces of revolution, and conic sections. We use the MINIMAL example as an instance of an isothermic surface with mean curvature zero (Figure 2.2b). As expected this surface exhibits the highest curvature line quality of all tested meshes. The error however cannot vanish completely since the surface's curvature field contains singularities. In the vicinity of these points the numerical curvature directions contain significant amounts of noise.

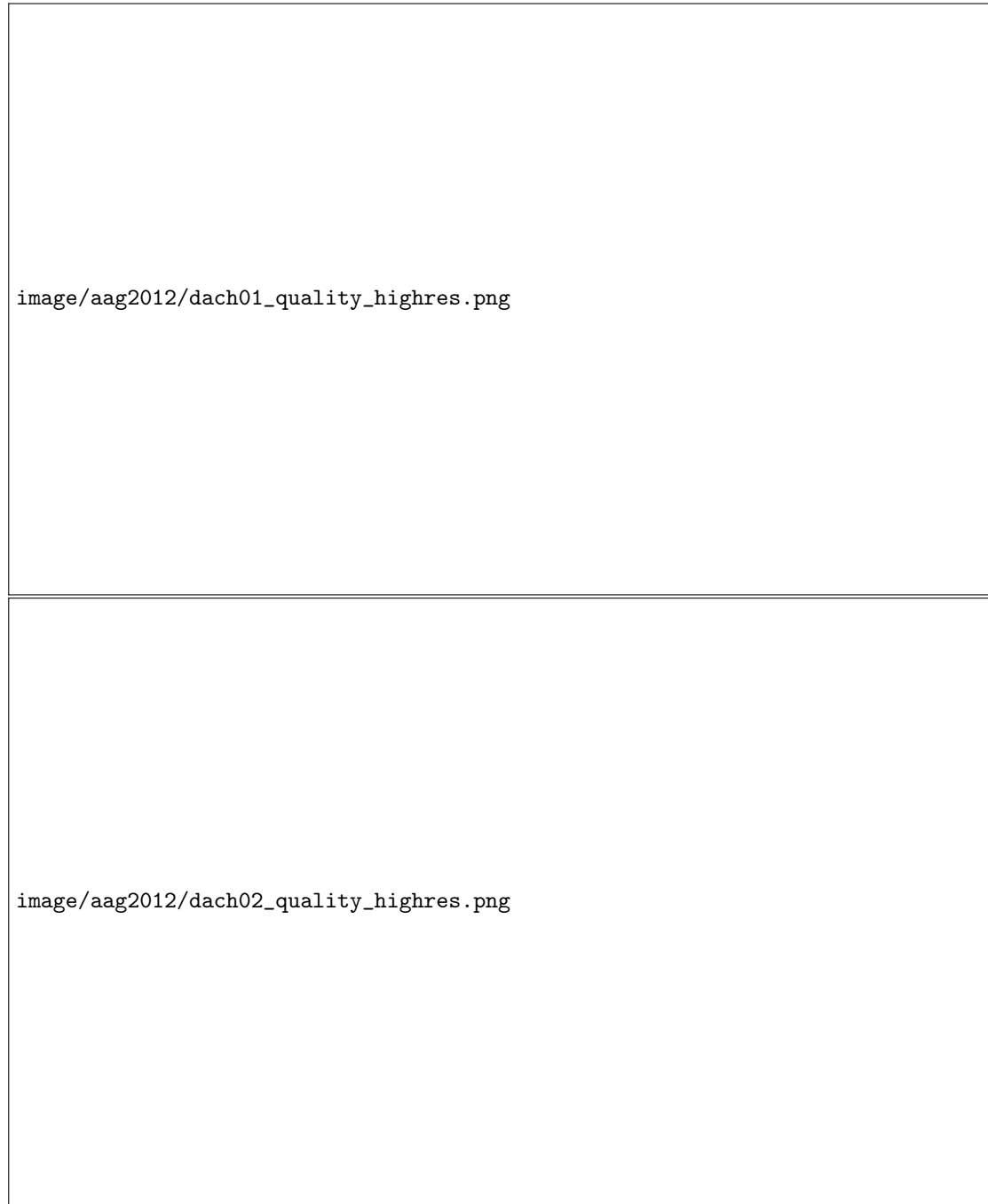


Figure 2.6: The quality of the parameterization is measured in radians per edge of the underlying triangulation. The checkerboard texture indicates the parameter lines of the map. Small (red and yellow) beads represent good curvature direction quality, big beads (green and blue) represent high deviation. The color of the histogram corresponds to the color of the beads. Note that the mean error of the ROOF surface (top) is half the error of the DOME. See also Table 2.1 for detailed quality measures of the other surfaces.

	$\#E$	$\#\partial E$	$Q_{\text{mean}}^\alpha$	$Q_{\text{max}}^\alpha$	$Q_\sigma^\alpha$
MINIMAL	6260	450	0.036	0.603	0.033
TEASER	17550	1000	0.057	1.20	0.066
ROOF	3766	470	0.051	0.610	0.059
DOME	1900	350	0.133	1.52	0.157

Table 2.1: The curvature line approximation quality of the examples.  $\#\partial E$  are the number of boundary edges.  $Q_\sigma^\alpha$  is the standard deviation of  $Q^\alpha$ .

**Non-isothermic surfaces.** Non-isothermic surfaces are surfaces that do not admit a parameterization with conformal curvature lines. We investigate the properties of surfaces (a), (c), and (d) displayed in Figure 2.2.

The TEASER surface was created as a minimizer of a spring functional fixing the boundary and modelling interior edges as springs of rest length zero. It is not far away from a minimal surface with the same boundary. The curvature line pattern however differs substantially as it contains singularities whereas the minimal surface with this boundary curve does not. The quality of the curvature line pattern is also very high. The mean angle error of the numerical directions is 3.2 degrees. Note that the deviation  $Q_\sigma$  from the mean value is also very low. For this surface the coordinates generated by our algorithm are a globally good approximation to conformal curvature lines.

A quality plot of the ROOF surface (Figures 2.2d and 2.5) is shown in Figure 2.6. Surprisingly, the quality of the curvature lines is as high as in the TEASER or the MINIMAL case. This suggests that a slight variation of the surface yields an isothermic surface. See also Figure 2.5 for a visual impression of the quality of the curvature lines.

The DOME model (Figure 2.2c) is created from a NURBS surface. The quality plot (Figure 2.6) reveals areas of high angle deviation especially around the singularities. Other areas, in particular those near the boundary, are of high curvature line quality. The distance to the nearest isothermic surface is expected to be larger than in the previous examples. More evidence for this is given in Section 2.1.5.

**Discussion.** Our parameterization scheme works well for surfaces that are not too far away from surfaces that possess isothermic coordinates. In the case of surfaces stemming from minimal or constant mean curvature surfaces we get almost perfect approximation quality of curvature lines. These are surfaces that are particularly interesting when designing beam layouts for roof structures that where form-found. For other surfaces the parameterization is conformal and the parameter line pattern captures the combinatorics of the curvature line pattern while approximating the curvature line geometry. There are of course surfaces for which our method is not applicable. If the boundary is too short compared to the overall size of the surface we cannot expect the solution to follow curvature lines as the distance to the boundary increases.

### 2.1.5 Discrete S-isothermic surfaces

Starting with a quasiisothermically parameterized mesh with low modulus we now aim to create discrete S-isothermic surfaces that stay in the vicinity of the input surface. S-isothermic surfaces were introduced by [BP99]: A quadrilateral mesh is *S-isothermic* if (i) all the quadrilaterals are planar, (ii) all faces have incircles, and (iii) the incircles of adjacent quadrilaterals touch. Figure 2.7 displays S-isothermic surfaces derived from our parametrizations shown in Figure 2.2.

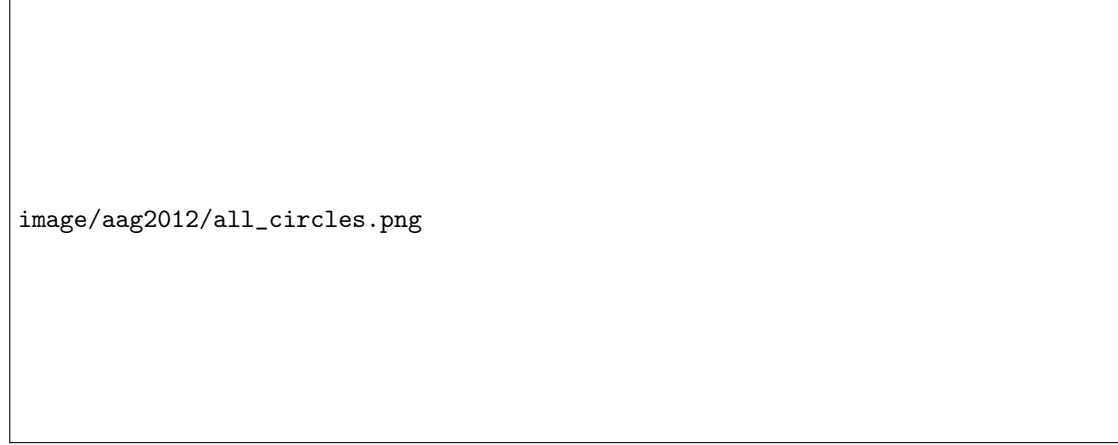


Figure 2.7: S-isothermic meshes created from the models presented in Figure 2.2. The inner quadrilaterals are optimized towards touching incircles. A series of touching circles in a row can be interpreted as discrete curvature line.

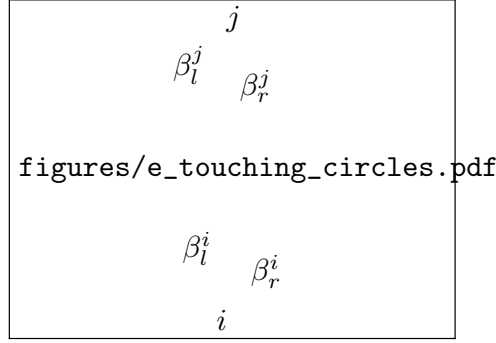


Figure 2.8: Labels for the touching-circles-functional at an edge. The circles touch if the ratio  $\cot(\beta^i/2) / \cot(\beta^j/2)$  is equal on both sides of the edge.

### Variational Principle

In this section we introduce an energy whose minimizers are S-isothermic surfaces. We denote quadrilaterals by  $ijklm \in F$  where the indices are in cyclic order. The S-isothermic energy  $E_S$  consists of three parts:

$$E_S := \lambda_1 E_{\text{planar}} + \lambda_2 E_{\text{incircle}} + \lambda_3 E_{\text{touch}} \quad (2.6)$$

The planarity energy  $E_{\text{planar}}$  penalizes non-planar quadrilateral faces. For each quad it can be defined either by the distance of the diagonals (an idea attributed to Peter Schröder in [PSB<sup>+</sup>08]) or the volume of the tetrahedron spanned by the four vertices. We give the formula for the former here.

$$E_{\text{planar}} = \sum_{ijklm \in F} \frac{\langle \Delta_{ji}, \Delta_{mj} \times \Delta_{ki} \rangle^2}{\|\Delta_{mj} \times \Delta_{ki}\|^2} \quad (2.7)$$

Here  $\Delta_{ij}$  is the vector pointing from vertex  $i$  to  $j$ .

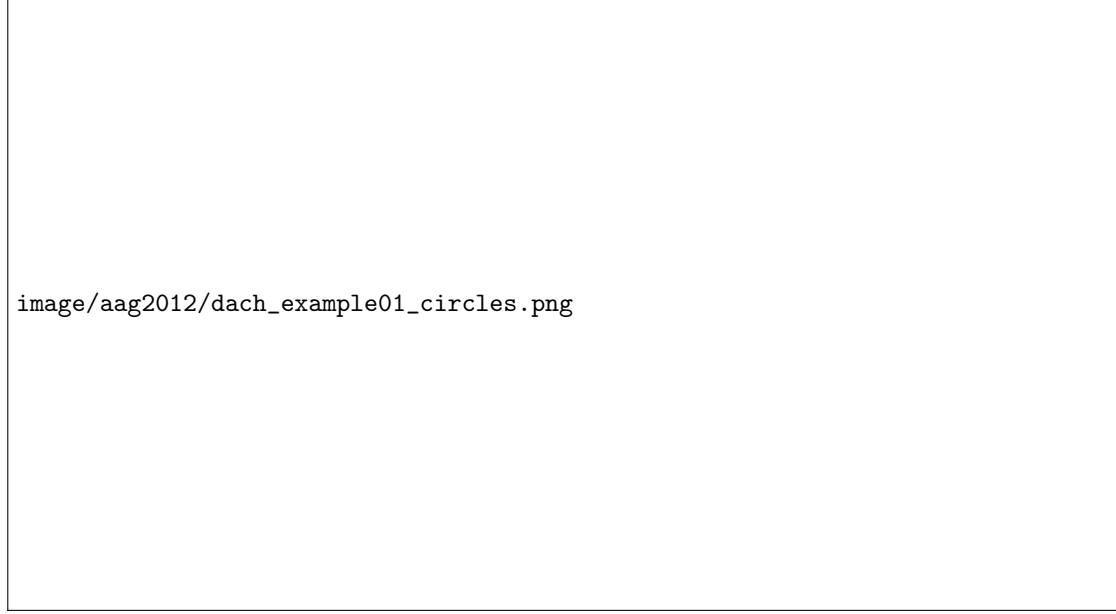


Figure 2.9: The S-isothermic circle packing on the ROOF model in detail.

For  $E_{\text{incircle}}$  we use the energy defined by [SHWP09] based on the fact that the sum of opposite edge lengths must be equal for a planar quad to possess an incircle.

$$E_{\text{incircle}} = \sum_{ijkm \in F} (l_{ij} + l_{km} - l_{jk} - l_{mi})^2 \quad (2.8)$$

The energy  $E_{\text{touch}}$  is a new energy that enforces touching incircles if faces are planar and possess incircles. It is defined per edge, see Figure 2.8 for the exact labeling of the angles at one edge. For an interior edge  $ij \in E$  we define

$$E_{\text{touch}}(ij) = \left( \cot \frac{\beta_l^j}{2} \cot \frac{\beta_r^i}{2} - \cot \frac{\beta_r^j}{2} \cot \frac{\beta_l^i}{2} \right)^2. \quad (2.9)$$

On boundary edges the energy is zero. All energies can be formulated in terms of the vertex coordinates and the derivatives can be calculated explicitly.

Since all energies are in general non-convex we need a good initial guess to find meaningful minimizers of  $E_S$ . S-isothermic minimal surfaces converge to isothermic parameterizations of smooth minimal surfaces [BHS06]. For general S-isothermic surfaces this is an open conjecture. The parameterizations obtained in Section 2.1.3 are good candidates to start from with the optimization of the functional. We use the non-linear optimization package PETSc/TAO [BBB<sup>+</sup>11, BMM<sup>+</sup>07] and its java binding [Som10] to find minimizers of  $E_S$ . Figure 2.10 shows convergence plots of  $E_S$  for the four models that were discussed in the previous section.

As seen in the quality analysis of Section 2.1.4, the TEASER, the MINIMAL, and the ROOF models are quasiisothermic surfaces with low modulus. For these models the corresponding S-isothermic surface is also close to the input surface. Figure 2.10 shows the energy during the optimization. Here the three close-to-isothermic meshes start with a lower energy than the DOME model.

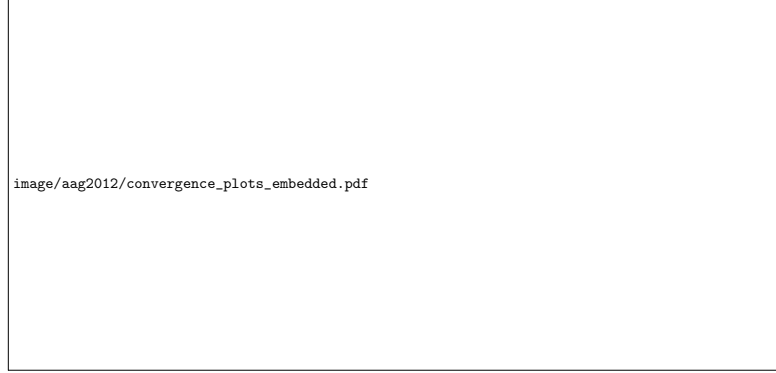


Figure 2.10: Convergence behavior of  $E_S$  during optimization. We use the meshes displayed in Figure 2.2 as initial guesses for the minimization. The convergence of the Teaser geometry is slower due to the high complexity.

After the DOME has passed some iterations it exhibits convergence properties similar to the other models. As this surface converges against a discrete S-isothermic surface, we observe a considerable change in shape during the first iterations especially around the singularities.

### Isometric Deformations of Minimal Surfaces

Every smooth minimal surface possesses a 1-parameter (associated) family of non-trivial isometric deformations. All surfaces in this family have the same Gauß map. For discrete S-isothermic minimal surfaces this construction is discretized in [BHS06]: Edge lengths and the conformality of the parameterization are preserved. We need to introduce the concept of dual surface to construct the family of isometric surfaces.

**The Dual Surface.** In differential geometry for isothermic surfaces there is a notion of a dual surface. This dual or Christoffel transform is also an isothermic surface. Both surfaces are parameterized with isothermic coordinates. This setup can be discretized using the definition of discrete S-isothermic surfaces. The dual surface can be constructed using the incircle structure of S-isothermic meshes. We introduce consistent signs on edges on a discrete S-isothermic surface such that opposite sides of the quads have the same sign and consecutive edges in a quad have different signs. The dual mesh of a mesh  $M$  will have parallel edges calculated as follows: Let  $e_{ij} = v_j - v_i$  be an edge vector of  $M$ . Then the dual edge vector  $e_{ij}^*$  satisfies the following equation:

$$e_{ij}^* = \pm \frac{1}{r_i \cdot r_j} e_{ij}$$

where  $r_i$  and  $r_j$  are the distances from the vertex  $v_i$  and  $v_j$  to the touching point of the incircles of incident faces at the edge  $e_{ij}$ . For a given discrete S-isothermic mesh we can easily calculate the dual mesh by enumerating the vertices along a spanning tree of edges. In Figure 2.13 the dual surface of the MINIMAL model is shown in the upper left hand corner. Via the dual surface we can now construct isometric deformations of minimal surfaces.

**Deformation.** The dual of a smooth minimal surface coincides with its Gauß map which is a part of a sphere. This sphere may be multiply covered. For discrete S-isothermic minimal surfaces this Gauß map is a part of a Koebe polyhedron, i.e., a polyhedral surfaces with edges



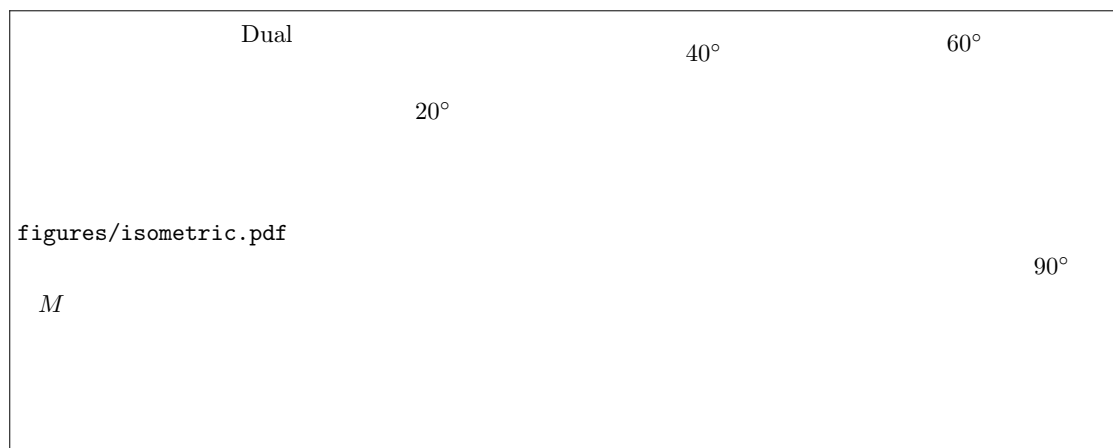


Figure 2.11: Non-trivial isometric deformations of a minimal surface. The edges of the dual surface are rotated to create a 1-parameter family of isometrically deformed surfaces with period  $2\pi$ . The histogram shows the edge length error of the  $90^\circ$  model when compared with the initial surface. The mean edge length deviation of this model is 1.28%.

tangent to a sphere. On the Koebe polyhedron every edge is rotated by a fixed angle in the tangent space of the sphere at the points of tangency of the edge. The resulting edge vectors again form closed quads and can be dualized. This dual surface has the same edge lengths as the initial minimal surface.

For minimal quad meshes with touching incircles that were created using our parameterization and the optimization step, the dual surface will be close to a Koebe polyhedron. We use a least-squares-sphere to define a consistent tangent space at the touching points of incircles with the edges. The resulting deformation of a given minimal surface is then close to isometric. To distribute the isometry error on the edges we average over different roots of the layout spanning tree. Surfaces that do not possess exact isometric deformations are deformed approximative.

We apply this procedure to the MINIMAL model (Figure 2.2a). Figure 2.13 shows the surface together with its dual and isometrically deformed versions with different turning angles.

### 2.1.6 Conclusions and Future Research

The main contributions of this article are, on the one hand, the definition of quasiisothermic parameterizations together with a new algorithm to compute parameterizations of surfaces that optimizes the corresponding quality measure. On the other hand, we have defined a new energy for meshes with touching incircles.

We see the main advantage of the algorithm presented in Section 2.1.3 in its simplicity and its applicability to shell-like roof structures which arise in architectural models. Since these models often have almost constant mean curvature and thus allow for an almost isothermic parameterization, our algorithm performs particularly well on these examples.

The new energy described in Section 2.1.5 is closely related to the article of [SHWP09] dealing with circle packing meshes. They explicitly do not treat quadrilateral meshes since they are aware of the shape restrictions and focus on triangle meshes instead. The shape restriction lies



Figure 2.12: Discrete S-isothermic ellipsoid

in the core of isothermic surfaces but did not influence our results dramatically for the surfaces in our focus. How to approximate arbitrary surfaces by isothermic surfaces is unknown and will be subject to future research. The results of Section 2.1.5 suggest that this might be possible using related methods.

Our new functional generates quad circle packing meshes in the sense of Schiftner *et al.*. For surfaces arising in architectural context (in particular for shell-like roofs) we are able to construct aesthetically pleasing quad meshes supporting a circle packing.

### 2.1.7 A discrete S-isothermic ellipsoid and its dual surface

Here we describe the construction of a discrete S-isothermic ellipsoid and its dual surface. (See [HJ03, p. 202] for the smooth analog). The rough construction outline is as follows. We start with a discretized version of the smooth isothermically parameterized ellipsoid. We obtain this by calculating a quasiisothermic parameterization of half of a triangulated ellipsoid. After remeshing the parameter lines are approximate curvature lines. We complete the surface by reflection at the boundary. Optimization of the S-isothermic functional yields the final discrete ellipsoid. Its dual surface is constructed as in Section 2.1.5.

The combinatorics at singularities of the discrete ellipsoid is not unique. If there is a discrete curvature line at the symmetry plane of the ellipsoid we have degenerate quads that have vertices with angle  $\approx \pi$ . The singularity is located at this valence 2 vertex. If there is no discrete curvature line at the symmetry plane then the singularity is located at the mid point of the edge connecting two valence three vertices. We have observed that the convergence behavior of the S-isothermic functional is considerable better in the former model of singularities. We therefore like to call only the discrete ellipsoid with curvature lines at symmetry planes a discrete ellipsoid.

## 2.2 Projective interpolation for arbitrary parameterizations

For discrete conformal maps [SSP08] take advantage of a remarkable property of discretely conformally equivalent meshes. Every triangle can be projectively mapped such that the circum



Figure 2.13: Dual surface of discrete S-isothermic ellipsoid of Figure 2.12.

circle is preserved. In fact this is a characterising property of discretely conformally equivalent meshes.

They argue that the circum circle preserving interpolation scheme gives visually better results especially for coarse meshes. We have observed that linear interpolation is a particularly bad choice at cone singularities of the parameterization (Figure 2.14 left).

Let  $M = (V, E, F)$  be a triangulated surface consisting of vertices  $i \in V$ , edges  $ij \in E$ . Let  $\lambda_{ij}$  be the logarithmic metric of the surface and  $\tilde{\lambda}_{ij}$  be the logarithmic metric of the domain of a parameterization. In general  $\lambda$  and  $\tilde{\lambda}$  are not discretely conformally equivalent. The system of linear equations

$$\lambda_{ij} + u_i + u_j = \tilde{\lambda}_{ij} \quad (2.10)$$

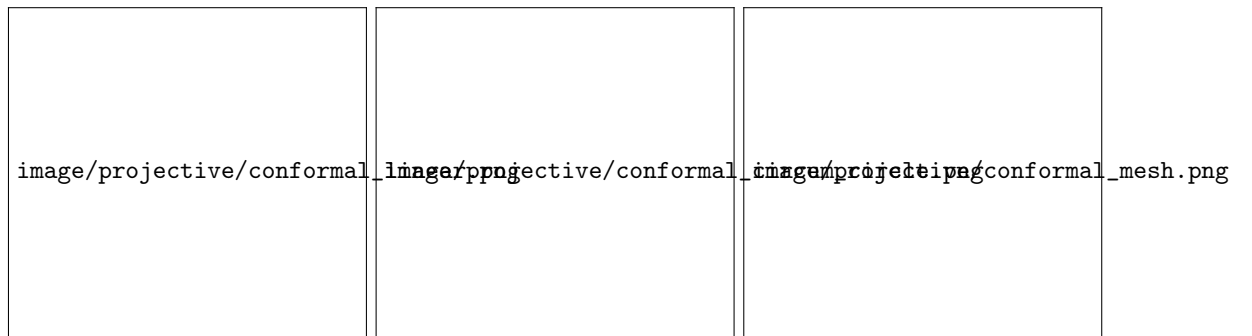


Figure 2.14: Linear (left) and circum circle preserving piece-wise projective (middle) interpolation at a cone-singularity of a coarse mesh (right) with vertices on a sphere. The parameterization is discrete conformal.

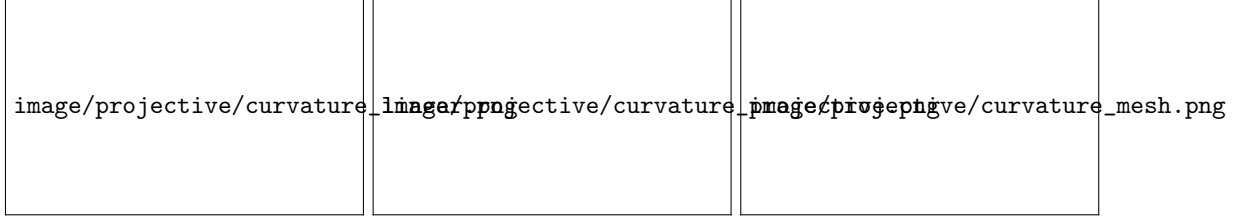


Figure 2.15: Linear (left) and piece-wise projective (middle) interpolation at a cone-singularity of a coarse mesh (right). The parameterization is not discrete conformal.

has no solution  $u \in \mathbb{R}^{|V|}$ . We can however solve this system in a least squares fashion such that

$$\sum_{ij \in E} \omega_{ij} (\lambda_{ij} + u_i + u_j - \tilde{\lambda}_{ij})^2$$

is minimal. Where  $\omega_{ij}$  is a weight per edge.

## 2.3 A variational principle for discrete Tschebyshev nets

Introduction...

### 2.3.1 Variational principle

Let  $M = (V, E, F)$  be a quad-mesh. The vertices of  $M$  are denoted by  $v_i \in V$ , the edges are  $e_{ij} \in E$ , and the quadrilaterals are denoted by  $f_{ijkl} \in F$ .

### 2.3.2 Energies

We use a linear combination of energies to enforce desired properties on the optimised mesh. Our energy consists of three parts.

$$E(M) = \lambda_1 E_{\text{ref}} + \lambda_2 E_{\text{len}} + \lambda_3 E_{\text{cur}} \quad (2.11)$$

The energy  $E_{\text{ref}}$  penalises the distance of vertices from a reference surface. This surface can be anything that gives a distance function, e.g., a triangulated surface or a NURBS-surface. The energy and its gradient are given by

$$\begin{aligned} E_{\text{ref}}(M) &= \sum_{v_i \in V} \langle v_i - cp_i, v_i - cp_i \rangle \\ \frac{\partial E_{\text{ref}}}{\partial v_i} &= 2(v_i - cp_i) \end{aligned}$$

Here  $v_i$  is a vertex of the optimised quad-mesh and  $cp_i$  a closest point on the reference surface measured from vertex  $v_i$ . The functional  $E_{\text{len}}$  measures edge length deviation from a given

reference length  $L$ . Its derivative and energy is given as

$$E_{\text{len}}(M) = \sum_{e_{ij} \in E} (\|v_i - v_j\| - L)^2$$

$$\frac{\partial E_{\text{len}}}{\partial v_i} = \sum_{e_{ij} \in \text{star}(v_i)} \left( 2 - \frac{2L}{\|v_i - v_k\|} \right) (v_i - v_k)$$

The sum in the derivative is taken over all edges incident to vertex  $v_i$ , called the edge-star of vertex  $v_i$ . The third energy is a fairing term that penalises a notion of curvature of curves on the surface. As we only deal with quad-meshes with  $\mathbb{Z}^2$  combinatorics every interior vertex has four adjacent edges. The energy  $E_{\text{cur}}$  and its gradient is defined as:

$$E_{\text{cur}}(M) = \sum_{v_i \in V} (\pi - \angle(e_{i1}, e_{i3}))^2 + (\pi - \angle(e_{i2}, e_{i4}))^2$$

$$\frac{\partial}{\partial v_j} \angle(e_{ij}, e_{ik}) = \frac{-1}{\|e_{ij}\|} \left( e_{ik} - e_{ij} \frac{\langle e_{ik}, e_{ij} \rangle}{\langle e_{ij}, e_{ij} \rangle} \right) \left\| e_{ik} - e_{ij} \frac{\langle e_{ik}, e_{ij} \rangle}{\langle e_{ij}, e_{ij} \rangle} \right\|^{-1}$$

$$\frac{\partial}{\partial v_i} \angle(e_{ij}, e_{ik}) = - \left( \frac{\partial}{\partial v_j} \angle(e_{ij}, e_{ik}) + \frac{\partial}{\partial v_k} \angle(e_{ij}, e_{ik}) \right)$$

Here and  $e_{i1}$ ,  $e_{i2}$ ,  $e_{i3}$ , and  $e_{i4}$  are the adjacent edges of  $v_i$  in cyclic order. An edge  $e_{ij}$  is also used in the role of a vector pointing from vertex  $v_i$  to vertex  $v_j$ .  $\angle(e_{ij}, e_{ik})$  is the angle spanned by the vectors  $e_{ij}$  and  $e_{ik}$ . From the angle derivatives with respect to the vertices the gradient can be computed efficiently.

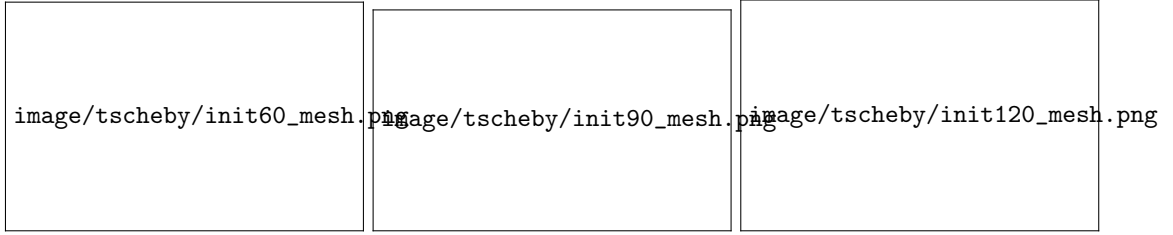


Figure 2.16: Different initialization shear angles for a conformal remesh.  $30^\circ$  left,  $0^\circ$  middle, and  $-30^\circ$  right.

### 2.3.3 Initialization and parameters

The energy  $E(M)$  is in general non-convex. That means there can be many local optima, and the solution found by some gradient descent depends on the initialisation. We propose to use a conformal remesh of the reference surface as initialization. The conformality of the parameterisation gives us control over the angles between edges of the quadrilaterals. We can introduce shear to the parameterisation and modify this angle globally. By this we start with meshes that have almost constant edge angle (see Fig. 2.16).

### 2.3.4 Implementation

We use the conformal mapping algorithm by [SSP08] to create the initial mesh. To minimize the energy  $E(M)$  we use the non-linear optimization package PETSc/TAO [BBB<sup>+</sup>11, BMM<sup>+</sup>07]

and its java binding [Som10]. We have made good experiences with normalising the energies to have gradient length one before optimization. Then we start with all  $\lambda$ s equal to one and modify them on the way if needed. If one encounters degenerate configurations during optimization one can drop the length energy term for a few iterations.

## Chapter 3

# Discrete Differential Geometry - Software Packages

In the field of Discrete Differential Geometry (DDG) there is a special need for experiments conducted with the help of computer software. Especially if the methods of DDG are applied to problems in computer graphics, geometry processing, or architecture, algorithms have to be implemented and convincing examples have to be presented. Additionally a suitable visualization of the results has to be included in a state-of-the-art publication.

There is a growing knowledge of software development in the mathematical community. This is partly due to the curricula of universities which started to include programming courses for undergraduate students. This enables the students to extend their abilities of creating visualizations and mathematical software, where former generations of students solely used Mathematica and MatLab.

This Chapter is the description and getting-started manual of a set of software packages (DDG Framework) written in Java. They are specifically designed for the creation of custom interactive software for experiments with algorithms and geometries treated within DDG. Section 3.1 introduces the JRWORKSPACE library of the JTEM project [jdt13b]. It is the foundation of any application created with the DDG Framework. It is also the user interface basis of JREALITY, a mathematical visualization library that uses JRWORKSPACE as plug-in and user interface tool [jdt13a]. In Section 3.3 we describe the software CONFORMALLAB. This package implements the methods of the publications [BPS10, Sec12, SRB12, BSS]. Section 3.4 introduces VARYLAB the software implementation of the methods described in the publications [LGSR11, LSRG12, SRB12]. This package is also released to partners of the development group as VARYLAB[GRIDSHELLS] or VARYLAB[ULTIMATE].

### 3.1 JRWORKSPACE - A plug-in driven GUI library

#### 3.1.1 Plug-ins

#### 3.1.2 Gui elements

#### 3.1.3 JRWORKSPACE and JREALITY

#### 3.1.4 Building a *jrworkspace* application

### 3.2 The JTEM libraries HALFEDGE and HALFEDGETOOLS

#### 3.2.1 The halfedge data structure and tools

#### 3.2.2 Data model and algorithms

### 3.3 CONFORMALLAB - Conformal maps and uniformization

#### 3.3.1 Embedded surfaces

#### 3.3.2 Elliptic and hyperelliptic surfaces

#### 3.3.3 Schottky data

#### 3.3.4 Surfaces with boundary

### 3.4 VARYLAB - Variational methods for discrete surfaces

#### 3.4.1 Functional plug-ins

#### 3.4.2 Implemented functionals and options

#### 3.4.3 Remeshing

### 3.5 U3D - 3D content in presentations and online publications

#### 3.5.1 3D content in PDF documents

### 3.6 Non-linear optimization with jPETSc/jTao

#### 3.6.1 A java wrapper for PETSc/Tao



# Bibliography

- [ACSD<sup>+</sup>03] Pierre Alliez, David Cohen-Steiner, Olivier Devillers, Bruno Lévy, and Mathieu Desbrun. Anisotropic polygonal remeshing. *ACM Trans. Graph.*, 22(3):485–493, 2003.
- [BBB<sup>+</sup>11] Satish Balay, Jed Brown, Kris Buschelman, William D. Gropp, Dinesh Kaushik, Matthew G. Knepley, Lois Curfman McInnes, Barry F. Smith, and Hong Zhang. PETSc Web page, 2011. <http://www.mcs.anl.gov/petsc>.
- [BHS06] Alexander I. Bobenko, Tim Hoffmann, and Boris Springborn. Minimal surfaces from circle patterns: geometry from combinatorics. *Ann. of Math. (2)*, 164(1):231–264, 2006.
- [BMM<sup>+</sup>07] Steve Benson, Lois Curfman McInnes, Jorge Moré, Todd Munson, and Jason Sarich. TAO user manual (revision 1.9), 2007. <http://www.mcs.anl.gov/tao>.
- [BP99] Alexander I. Bobenko and Ulrich Pinkall. Discretization of surfaces and integrable systems. In *Discrete integrable geometry and physics (Vienna, 1996)*, volume 16 of *Oxford Lecture Ser. Math. Appl.*, pages 3–58. Oxford Univ. Press, New York, 1999.
- [BPS10] Alexander I. Bobenko, Ulrich Pinkall, and Boris Springborn. Discrete conformal maps and ideal hyperbolic polyhedra. Preprint; <http://arxiv.org/abs/1005.2698>, 2010.
- [BS08] Alexander I. Bobenko and Yuri B. Suris. *Discrete differential geometry – Integrable structure*, volume 98 of *Graduate Studies in Mathematics*. American Mathematical Society, Providence, RI, 2008.
- [BSS] Alexander I. Bobenko, Stefan Sechelmann, and Boris Springborn. Uniformization of discrete Riemann surfaces. in preparation.
- [CSM03] David Cohen-Steiner and Jean-Marie Morvan. Restricted Delaunay triangulations and normal cycle. In *Symposium on Computational Geometry*, pages 312–321, 2003.
- [FH05] M. S. Floater and K. Hormann. Surface parameterization: a tutorial and survey. In N. A. Dodgson, M. S. Floater, and M. A. Sabin, editors, *Advances in Multiresolution for Geometric Modelling*, Mathematics and Visualization, pages 157–186. Springer, Berlin, Heidelberg, 2005.
- [Guo11] Ren Guo. Combinatorial yamabe flow on hyperbolic surfaces with boundary. *Commun. Contemp. Math.*, 13(5):827–842, 2011.

- [HJ03] Udo Hertrich-Jeromin. *Introduction to Möbius Differential Geometry*. London Mathematical Society Lecture Note Series. Cambridge University Press, 2003.
- [jdt13a] jReality developer team. JREALITY website, 2013. <http://www.jreality.de>.
- [jdt13b] jTEM developer team. JTEM website, 2013. <http://www.jtem.de>.
- [Jos07] Jürgen Jost. *Compact Riemann Surfaces*. Universitext (En ligne). Springer-Verlag Berlin Heidelberg, 2007.
- [KNP07] Felix Kälberer, Matthias Nieser, and Konrad Polthier. Quadcover - surface parameterization using branched coverings. *Comput. Graph. Forum*, 26(3):375–384, 2007.
- [LGSR11] Elisa Lafuente Hernández, Christoph Gengnagel, Stefan Sechelmann, and Thilo Rörig. On the materiality and structural behaviour of highly-elastic gridshell structures. In C. Gengnagel, A. Kilian, N. Palz, and F. Scheurer, editors, *Computational Design Modeling: Proceedings of the Design Modeling Symposium Berlin 2011*, pages 123–135. Springer, 2011.
- [LPW<sup>+</sup>06] Yang Liu, Helmut Pottmann, Johannes Wallner, Yong-Liang Yang, and Wenping Wang. Geometric modeling with conical meshes and developable surfaces. *ACM Trans. Graph.*, 25(3):681–689, 2006.
- [LSRG12] Elisa Lafuente Hernández, Stefan Sechelmann, Thilo Rörig, and Christoph Gengnagel. Topology optimisation of regular and irregular elastic gridshells by means of a non-linear variational method. In L. Hesselgren, S. Sharma, J. Wallner, N. Baldassini, P. Bompas, and J. Raynaud, editors, *Advances in Architectural Geometry 2012*, pages 147–160. Springer, 2012.
- [Luo04] Feng Luo. Combinatorial yamabe flow on surfaces. *Commun. Contemp. Math.*, 6(5):765–780, 2004.
- [PLW<sup>+</sup>07] Helmut Pottmann, Yang Liu, Johannes Wallner, Alexander Bobenko, and Wenping Wang. Geometry of multi-layer freeform structures for architecture. *ACM Trans. Graph.*, 26(3), July 2007.
- [PSB<sup>+</sup>08] Helmut Pottmann, Alexander Schiftner, Pengbo Bo, Heinz Schmiedhofer, Wenping Wang, Niccolo Baldassini, and Johannes Wallner. Freeform surfaces from single curved panels. *ACM Trans. Graph.*, 27(3):#76, 1–10, 2008.
- [SdS01] A. Sheffer and E. de Sturler. Parameterization of Faceted Surfaces for Meshing using Angle-Based Flattening. *Engineering with Computers*, 17:326–337, 2001.
- [Sec12] Stefan Sechelmann. Uniformization of discrete Riemann surfaces. In *Oberwolfach Reports*, 2012.
- [SHWP09] Alexander Schiftner, Mathias Höbinger, Johannes Wallner, and Helmut Pottmann. Packing circles and spheres on surfaces. *ACM Trans. Graphics*, 28(5):#139,1–8, 2009. Proc. SIGGRAPH Asia.
- [Som10] Hannes Sommer. jPETScTao JNI library web page, 2010. <http://jpetsctao.zwoggel.net/>.

- [SPR06] Alla Sheffer, Emil Praun, and Kenneth Rose. Mesh parameterization methods and their applications. *Foundations and Trends in Computer Graphics and Vision*, 2(2):105–171, 2006.
- [Spr09] Boris Springborn. Discrete conformal equivalence for triangle meshes. In *Oberwolfach Reports*, volume 6 of *Oberwolfach Reports*, pages 104–106, 2009.
- [SRB12] Stefan Sechelmann, Thilo Rörig, and Alexander I. Bobenko. Quasiisothermic mesh layout. In L. Hesselgren, S. Sharma, J. Wallner, N. Baldassini, P. Bompas, and J. Raynaud, editors, *Advances in Architectural Geometry 2012*, pages 243–258. Springer, 2012.
- [SSP08] Boris Springborn, Peter Schröder, and Ulrich Pinkall. Conformal equivalence of triangle meshes. *ACM Trans. Graph.*, 27(3):77:1–77:11, August 2008.
- [ZSW10] Mirko Zadavec, Alexander Schiftner, and Johannes Wallner. Designing quad-dominant meshes with planar faces. *Computer Graphics Forum*, 29(5):1671–1679, 2010. Proc. Symp. Geometry Processing.



# Acknowledgements